Probing Elasticity at the Nanoscale: Terahertz Acoustic Vibration of Small Metal Nanoparticles

ARTICLE *in* NANO LETTERS · MAY 2010

Impact Factor: 13.59 · DOI: 10.1021/nl100604r · Source: PubMed

7 AUTHORS, INCLUDING:

Vincent Juvé
Université du Maine
18 PUBLICATIONS **293** CITATIONS
SEE PROFILE

Aurélien Crut
Claude Bernard University Lyon 1
39 PUBLICATIONS **899** CITATIONS
SEE PROFILE

NANO LETTERS

pubs.acs.org/NanoLett

Probing Elasticity at the Nanoscale: Terahertz Acoustic Vibration of Small Metal Nanoparticles

Vincent Juvé, Aurélien Crut, Paolo Maioli,* Michel Pellarin, Michel Broyer, Natalia Del Fatti, and Fabrice Vallée

Université Lyon 1, CNRS, LASIM, 43 bd du 11 Novembre 1918, 69622 Villeurbanne cedex, France

ABSTRACT The acoustic response of surface-controlled metal (Pt) nanoparticles is investigated in the small size range, between 1.3 and 3 nm (i.e., 75−950 atoms), using time-resolved spectroscopy. Acoustic vibration of the nanoparticles is demonstrated, with frequencies ranging from 1.1 to 2.6 THz, opening the way to the development of THz acoustic resonators. The frequencies, measured with a noncontact optical method, are in excellent agreement with the prediction of a macroscopic approach based on the continuous elastic model, together with the bulk material elastic constants. This demonstrates the validity of this model at the nanoscale and the weak impact of size reduction on the elastic properties of a material, even for nanoparticles formed by less than 100 atoms.

KEYWORDS Nanoacoustics, THz resonators, elasticity, nanomechanics, time-resolved measurements, platinum clusters

The impact of size reduction on the acoustic response of a nanoobject is currently attracting considerable interest. This is motivated by fundamental issues, i.e., the impact of size on the elastic properties of a nanoobject, and by technological ones, i.e., the development of high-frequency Terahertz nanoresonators and nanoelectromechanical systems (NEMS) for application as high-sensitivity sensors or optomechanical transducers. Reaching the Terahertz domain requires reduction of the size of the resonators down to a few nanometers, together with maintaining a sufficiently high quality factor of the mechanical resonance.[1] In this context, key technological and fundamental issues are the impact of size reduction on the elastic properties of a material and the validity of the continuum mechanics model used for describing resonators at the nanoscale. These two ingredients that form the macroscopic model of the acoustic response of a nanoobject become highly questionable for objects formed by a few hundred atoms, where surface effects due to uncoordinated surface atoms should become important.[2−4]

Modification of the elastic properties of a material at the nanoscale has been extensively investigated in semiconductor[5−7] and metal[8−10] nanowires using various mechanical, electromechanical, or optical methods. However, even for the relatively large sizes investigated up to now (larger than about 20 nm), the experimental results led to different conclusions, i.e., stiffening, softening, or no modification of the material properties with size reduction. These discrepancies can be ascribed to the different boundary conditions imposed to the nanoobjects (e.g., fixed or free ends) and to artifacts due to surface contaminants or oxidation. In contrast, experiments performed on nanospheres have suggested either no impact of size reduction on the material elastic properties (nanospheres with diameters down to 3 nm for gold and silver samples,[11−14] and down to 2.3 nm for ZnO nanoparticles[15]) or a molecular-type response (thiol-capped gold nanoparticles with size ranging from 1.1 to 2.2 nm[16]). Though the size effect can be material dependent, dispersion of the experimental results raises the question of the impact of the measurement procedure on the obtained data and of the nanoobject surface condition. These issues have precluded unambiguous determination of the intrinsic size effect on the elastic properties of a nanomaterial.

In this context, optical experimental methods such as time-resolved[11,12] or Raman[14] spectroscopies offer the key advantages of requiring no contact and permitting investigation of very small objects without manipulating them during sample preparation. Nanoobjects in a liquid or solid matrix or deposited on a substrate can thus be studied, avoiding any spurious effect due to mechanical contact. We have used here time-resolved optical spectroscopy to investigate the acoustic vibration of small metal nanoparticles (particles with diameter ranging from 1.3 to 3 nm). Platinum particles were chosen as a model system as they are free from oxidation effects and their acoustic vibration can be efficiently excited in the time domain (see below). This experimental method gives selectively access to the fundamental acoustic breathing mode, whose characteristics directly reflect the elastic properties of the particles.

In the small size regime of interest here, a large fraction of the atoms forming the particles are at their surface (more than 50% for nanospheres smaller than 3 nm). Care must be taken to control their surface conditions and to determine their intrinsic properties. Quasi-spherical platinum nanopar-

* Corresponding author, pmaioli@lasim.univ-lyon1.fr.

Received for review: 2/19/2010
Published on Web: 04/22/2010

DOI: 10.1021/nl100604r | *Nano Lett.* **2010,** *10,* 1853–1858

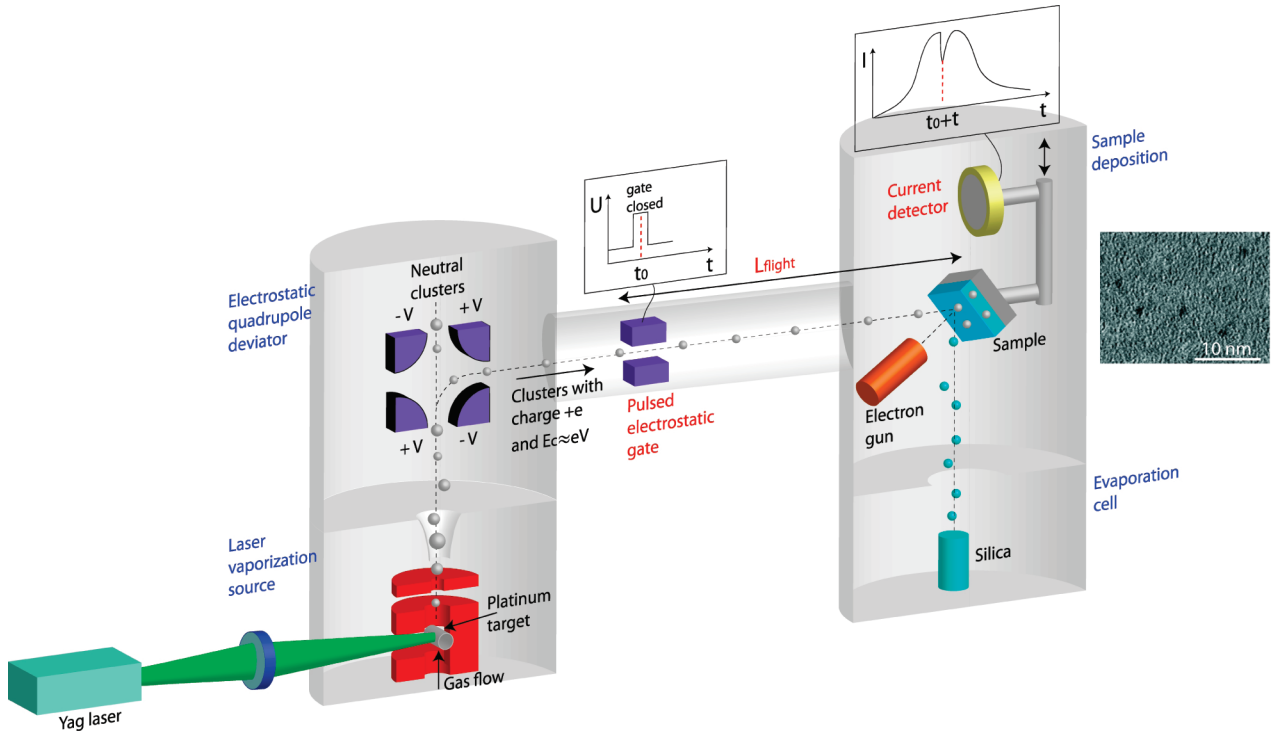

FIGURE 1. Synthesis of mass-selected platinum nanoparticles using LECBD. Platinum clusters produced by pulsed laser ablation are energy-selected with a quadrupole deflector (only the clusters with kinetic energy $E_c \approx eV$ are deflected by about 90°). The velocity of the selected clusters is determined by measuring their time-of-flight between a pulsed electronic gate and a current detector put at the sample position. To produce the sample, the clusters are deposited on a substrate and neutralized using an electron gun. They are either embedded in a matrix by codeposition of silica or deposited on the substrate surface. A TEM image of Pt nanoparticles with a mean diameter of 1.5 nm is shown on the right-hand side.

ticles with contaminant-free surfaces were thus synthesized by physical means, i.e., using a low energy cluster beam deposition (LECBD) apparatus associated to a quadrupole cluster mass selector[17] (Figure 1). This system is based on a vaporization laser source using a nanosecond frequency-doubled pulsed Nd^{3+}:YAG laser.[18] The metallic plasma created by focusing the laser on a 99.9% purity platinum target is rapidly cooled by collisions with an inert gas (helium) flowing in the growth chamber. This induces nucleation and growth of small metal clusters whose average size can be changed in the 1 to 5 nm diameter range by adjusting the gas pressure. The cluster/gas mixture subsequently expands through a conical nozzle into the high vacuum chamber to form a supersonic beam. Positively singly charged clusters (about 5% of the overall cluster population) with a given kinetic energy are selected out of this beam by deflecting them at right angles with an electrostatic quadrupolar deviator. As the velocity dispersion is weak, this selection in kinetic energy translates into a mass selection of the clusters, i.e., a size selection. The mass dispersion of the selected clusters is ±15% of their average mass, which corresponds to a ±5% dispersion of their average size, as compared to about ±25 to ±40% for nonselected clusters.[17] The nanoparticle characteristics were checked by transmission electron microscopy (TEM) after their deposition on a TEM grid. The samples used in our experiments were formed by nanoparticles deposited on a 1 mm thick Suprasil substrate with or without embedding them into a silica matrix (Figure 1). During deposition the size-selected charged clusters are neutralized by an electron beam. The kinetic energy per atom of the clusters is sufficiently weak to avoid their fragmentation upon impact on the surface.[18] The volume fraction of metal in the deposited films is in the 5×10^{-4} to 2×10^{-2} range for cluster mean diameters ranging from 1.3 to 3 nm (corresponding to a metal equivalent thicknesses of 0.5−1 nm). These low volume fractions ensure negligible nanoparticle coalescence after deposition, and avoid optical interactions between nanoparticles. As compared to chemical synthesis methods, the main advantage of this technique is to permit preparation of narrow size-distribution nanoparticles with surfaces free from surfactant molecules. It also permits direct testing of the impact of the environment on their acoustic response, performing measurements on the same particles with or without embedding silica matrix (i.e., using a mask to deposit silica on only part of the sample).

The elastic response of the platinum nanoparticles was investigated via measuring the properties of their fundamental breathing mode using a femtosecond optical pump−probe technique.[19] In this approach a first pump pulse excites the conduction electrons of the nanoparticle. A second time-delayed probe pulse follows the change of the sample optical transmission $\Delta T/T$, yielding information on

DOI: 10.1021/nl100604r | *Nano Lett.* **2010,** *10,* 1853–1858

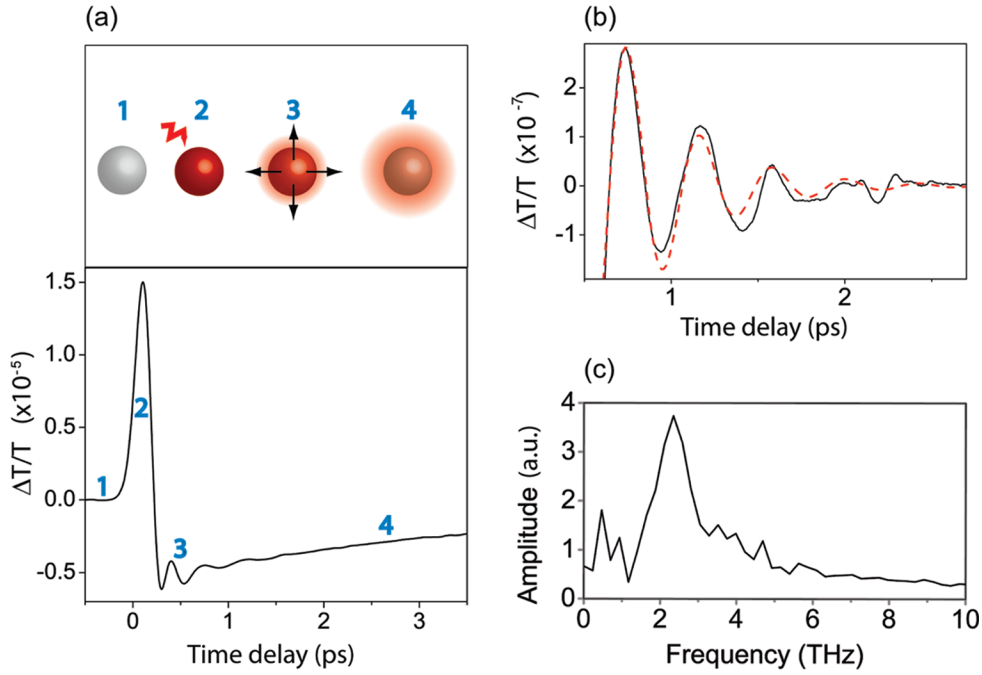

FIGURE 2. (a) Change of the sample probe transmission $\Delta T/T$ as a function of the pump−probe delay measured in silica-embedded 1.5 nm platinum nanoparticles (bottom). The time sequence of the observed processes is illustrated in the upper panel: nanosphere at thermal equilibrium (1), its ultrafast electron excitation by the pump pulse and electron−lattice thermalization (2), its acoustic vibration (3) and its cooling by energy transfer to its environment (4). (b) Oscillating part of the $\Delta T/T$ signal shown in (a), together with a fit by a damped sinusoidal function (red line). Its Fourier transform is shown in (c).

electron energy relaxation processes and on the mechanical movement of the particles (Figure 2).[19] The experimental setup is based on a homemade Ti:sapphire oscillator delivering pulses of about 20 fs with a wavelength of 840 nm at a repetition rate of 76 MHz. The output pulse train is split into two parts, one being frequency-doubled to 420 nm in a 200 μm thick BBO crystal. The two (fundamental and harmonic) beams are focused on the sample using two different lenses. The fundamental pulse at 840 nm is used as the pump pulse. The time-dependent relative transmission change $\Delta T/T$ of the sample induced by the pump beam is monitored at 420 nm, using the second frequency-doubled beam. The time delay between the pump and probe pulses is varied using a mechanical delay stage. High sensitivity detection of the pump-induced changes of the probe pulse transmission is achieved by mechanical chopping of the pump beam at 100 kHz, and lock-in detection of the probe beam transmission change.

The probe transmission change $\Delta T/T$ signal measured using this high-sensitivity two-color pump−probe setup is illustrated in Figure 2a in the case of 1.5 nm diameter Pt particles embedded in silica. The fast $\Delta T/T$ rise and fall on a few hundred femtosecond time scale reflects both the instantaneous nonresonant response of the silica substrate and excitation of the nanoparticles. The former is due to the nonlinear response of silica[20] and will not be discussed here. The latter reflects heating of the nanoparticle electrons by the pump pulse and their subsequent cooling by electron−lattice interaction in each particle (process 2 in Figure 2a). This leads to electron−lattice thermalization within each particle, with a characteristic time constant of the order of 200 fs, faster than in the commonly studied gold or silver nanoparticles.[21] The resulting ultrafast heating of the lattice launches the dilation of the particles, which subsequently undergo radial contractions and expansions around their new equilibrium size.[11,13] This motion corresponds to in-phase launching of the fundamental breathing mode of the particles, i.e., their isotropic volume oscillations, which corresponds to the fundamental mode of a mechanical resonator.[11,13] This mechanical movement induces a periodic modulation of the metal dielectric function, which shows up by oscillations of the differential probe transmission $\Delta T/T$ on a picosecond time scale (process 3 in Figure 2a).[11,13,19] The oscillations overlap with a background signal due to the overall heating of the nanoparticle, the latter contribution slowly decaying as the particle cools down by transferring its energy to the surrounding matrix (process 4 in Figure 2a).[22]

We will focus here on the oscillating part of the signal that reflects the nanoparticle acoustic breathing movement. This is more clearly seen after subtraction of the background signal (Figure 2b). The period T_0 of the oscillations is determined either by fitting the oscillating part of the signal in the time domain with a damped sinusoidal function (Figure 2b) or by Fourier transforming it (Figure 2c).[23] The two methods lead to the same period $T_0 \approx 440 \pm 20$ fs for the 1.5 nm diameter silica-embedded

DOI: 10.1021/nl100604r | *Nano Lett.* **2010,** *10,* 1853–1858

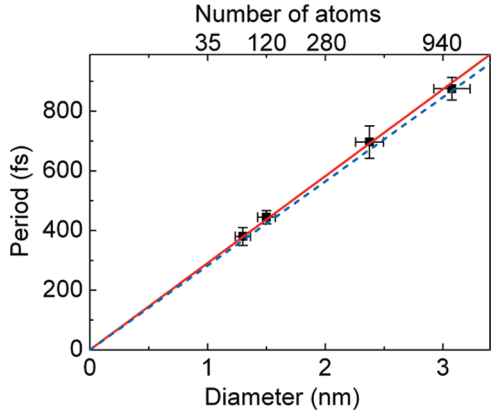

FIGURE 3. Period of the acoustic vibrations measured in Pt nanoparticles as a function of their mean diameter (the corresponding number of atoms is shown on the top axis). The horizontal error bars correspond to the particle size dispersion and the vertical ones to the standard deviation of measurements performed in different parts of a sample. The lines are computed using continuum elasticity theory with the bulk elastic constants of platinum, considering nanospheres either embedded in silica (dashed blue line) or free (solid red line).

platinum nanoparticles. Identical results were obtained for nonencapsulated nanoparticles, indicating that the silica matrix has a negligible impact on the period of the observed vibration. The observed oscillation decay is similar in silica embedded and nonencapsulated particles, suggesting that it is dominated by inhomogeneous damping, i.e., dephasing of the initially in phase acoustic movement of the different nanoparticles due to their size and shape dispersions.[11,24]

Similar measurements were performed in different samples with mean nanoparticle diameters of 3, 2.4, 1.5, and 1.3 nm (i.e., formed by about 940, 480, 120, and 75 atoms, respectively). The observed oscillation period increases with the particle size (Figure 3), in stark contrast with recent results obtained in chemically synthesized small gold nanoparticles covered by thiols (size independent $\Delta T/T$ oscillation periods were observed for nanoparticles with mean diameter in the 2.2 to 1.1 nm range[16]). This further stresses the impact of the particle interface conditions on the measured response of small nanoobjects. The measured oscillation frequency ranges from 1.1 to 2.6 THz. These results demonstrate that artificial acoustic nanoresonators with a given resonant frequency in the Terahertz range can be created and efficiently excited by optical means.

The oscillation periods measured in the different samples show a linear increase with the mean diameter of the nanoparticles (Figure 3). This behavior and the measured values of the periods are in excellent agreement with the fundamental radial mode frequencies computed using the macroscopic approach. This corresponds to computing the acoustic modes of an elastically isotropic homogeneous sphere embedded in a homogeneous isotropic matrix using continuum mechanics[25−27] with the elastic constants of the bulk material. This approach, first developed for macroscopic objects,[25,26] corresponds to solving the Navier equation with the proper boundary conditions, i.e., imposing continuity of displacement and stress at the sphere−matrix interface. This leads to the following expression for the complex frequency $\tilde{\omega}_0 = \omega_0 + i\Gamma$ of the fundamental breathing mode of a sphere of diameter D

$$\frac{x_R}{\tan(x_R)} = 1 - \frac{{x_R}^2}{\eta}\frac{1 + i\dfrac{x_R}{\alpha}}{{x_R}^2 + 4(\alpha\gamma)^2\left(\dfrac{1}{\eta\beta^2} - 1\right)\left(1 + i\dfrac{x_R}{\alpha}\right)} \quad (1)$$

where x_R is the reduced complex frequency, $x_R = \tilde{\omega}_0 D/2{c_L}^s$. The constants α, β, γ, and η are set by the sphere and matrix elastic properties: $\alpha = {c_L}^m/{c_L}^s$, $\beta = {c_T}^m/{c_T}^s$, $\gamma = {c_T}^m/{c_L}^m$, and $\eta = \rho^m/\rho^s$, where ${c_L}^{s,m}$ and ${c_T}^{s,m}$ are the longitudinal and transverse sound velocities of the material forming the sphere (superscript s) and matrix (superscript m), and $\rho^{s,m}$ their densities. Equation 1 is numerically solved to compute the reduced frequency and thus the period of the breathing mode

$$T_0 = 2\pi/\omega_0 = t_0 D/{c_L}^s \quad (2)$$

The reduced period t_0 is set by the sound velocities and densities of the sphere and environment materials. Using the tabulated bulk elastic constants of platinum (Young's modulus 168 GPa, Poisson's ratio 0.377, and density 21 450 kg/m^3) a t_0 value of about 1.1 is obtained for free spheres. This value yields an excellent quantitative reproduction of the mode periods measured in time-resolved experiments (Figure 3, where no fitting parameter has been used). For embedded particles, ω_0 and thus t_0 are almost matrix independent if the acoustic mismatch between the materials forming the sphere and the matrix is large.[25,27] This is the case for platinum nanospheres embedded in silica. The period T_0 computed from eq 1 is reduced by only about 3% for silica-embedded Pt nanospheres as compared to free ones (Figure 3). This is consistent with the fact that identical experimental results were obtained for samples with or without silica encapsulation, confirming the weak role of the environment in our experiment.

For all the studied samples the observed decay time of the oscillations is dominated by inhomogeneous damping.[11,24] This is consistent with the large acoustic impedance mismatch of platinum and silica, leading to a relatively small homogeneous damping, i.e., due to acous-

DOI: 10.1021/nl100604r | *Nano Lett.* **2010,** *10,* 1853–1858

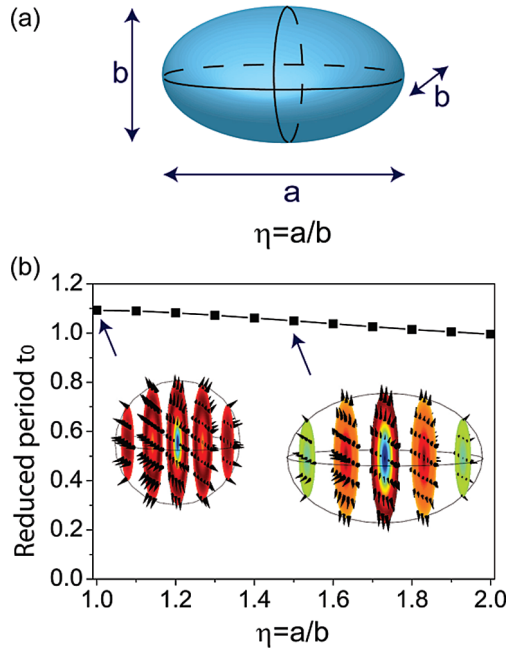

FIGURE 4. Computed reduced period $t_0 = T_0 c_L^s / D_{eq}$ of the breathing acoustic mode of a prolate platinum ellipsoid as a function of its aspect ratio $\eta = a/b$ for a fixed equivalent diameter D_{eq}. The ellipsoid geometry is shown on the left-hand side, and its equivalent diameter is defined by $D_{eq} = (ab^2)^{1/3}$.

tic energy transfer to the surrounding matrix.[24] The contribution of this effect is thus difficult to experimentally estimate in our samples but could be determined in other metal−matrix systems exhibiting better acoustic matching, such as silver−silica. Such study would permit a further test of the prediction of the macroscopic acoustic model in the small size regime and yield information on the limit of the quality factor of nanoresonators.

The experimental results might be influenced by deviation of the investigated particle shape from sphericity or by crystallinity defects. To test the impact of the former effect, we have computed the breathing mode period of an elliptical Pt nanoparticle with the macroscopic model and using a finite element analysis.[28] Increasing the aspect ratio η of an ellipsoid of fixed volume (or equivalent diameter D_{eq}, Figure 4a) from that of a sphere, $\eta = 1$, to that of a prolate ellipsoid, $\eta = 1.5$, the breathing mode period decreases by only about 4% (Figure 4b). The assumed deviation from sphericity is larger than the experimental one in our samples, leading to the conclusion that the nanosphere model is an excellent approximation here. These results are consistent with previously reported simulations in noble metal particles that have shown that deviation from sphericity has a weak impact on the fundamental breathing mode period of nanoparticles.[28] With the same numerical approach, the impact of crystallinity defects has been estimated by computing the breathing mode period assuming either a polycrystalline or monocrystalline nanoparticle. In the former case the direction-averaged elastic constants were used, while the elastic constants of the cubic crystal were used in the latter (these were derived from the bulk polycrystalline constants using a Zener's anisotropy ratio of 1.6 for platinum, as suggested by experimental measurements[29] and formulas relating polycrystalline and monocrystalline elastic constants[28]). The loss of anisotropy of the displacement profile does not significantly affect the reduced periods of the fundamental breathing mode, which differ by only 0.2% between a polycrystalline and monocrystalline nanoparticle.

In conclusion, using noncontact time-resolved spectroscopy, we have investigated the acoustic vibration of surface-controlled platinum nanoparticles prepared by a physical method. The results clearly demonstrate that, in contrast to many previous experimental reports, the mechanical vibration of a metal object is very well described by the macroscopic approach down to the 1 nm size range, i.e., for particles formed by less than 100 atoms. Furthermore, no size-induced modification of the material elastic properties has been observed even for 75 atom particles. These first experimental results in the very small size range constitute an important input for modeling the mechanical properties of a metal at the nanoscale. Furthermore, they demonstrate that selective excitation and detection of the acoustic vibration of small metallic objects in the one-nanometer size range can be achieved. This opens up the possibility of creating optically driven resonators or acoustic wave generators in the Terahertz domain.

This investigation also raises new perspectives for experimentally addressing the influence of the nature of bonding on the acoustic properties of small particles by comparing different materials. In particular, time-resolved techniques are also applicable to the investigation of the acoustic response of semiconductor nanoparticles.[30] Their extension to the small size regime in these systems would be particularly interesting, since molecular dynamics simulations predict a significant deviation of the acoustic response of nanoobjects in the case of covalent Si or Ge compounds formed by less than 500 atoms[31,32] (which corresponds to diameters of 2.6 and 2.8 nm), while small effects are indicated for nanospheres of ionocovalent material (ZnO, diameter 1.5 nm[2,33]).

Acknowledgment. M. Broyer and N. Del Fatti acknowledge support by the Institut Universitaire de France (IUF). This work was funded by the "Opthermal" grant of the Agence Nationale de la Recherche.

REFERENCES AND NOTES

(1) Pelton, M.; Sader, J. E.; Burgin, J.; Liu, M.; Guyot-Sionnest, P.; Gosztola, D. *Nat. Nanotechnol.* **2009**, *4*, 492–495.
(2) Combe, N.; Saviot, L. *Phys. Rev. B* **2009**, *80*, No. 035411.
(3) McDowell, M. T.; Leach, A. M.; Gall, K. *Nano Lett.* **2008**, *8*, 3613–3618.
(4) Park, H.; Klein, P. *J. Mech. Phys. Solids* **2008**, *56*, 3144–3166.
(5) Wong, E. W.; Sheehan, P. E.; Lieber, C. M. *Science* **1997**, *277*, 1971–1975.

DOI: 10.1021/nl100604r | *Nano Lett.* **2010,** *10,* 1853–1858

(6) Poncharal, P.; Wang, Z. L.; Ugarte, D.; de Heer, W. A. *Science* **1999***283*, 1513–1516.
(7) Chen, C.; Shi, Y.; Zhang, Y.; Zhu, J.; Yan, Y. *Phys. Rev. Lett.* **2006**, *96*, No. 075505.
(8) Staleva, H.; Hartland, G. V. *Adv. Funct. Mater.* **2008**, *18*, 3809–3817.
(9) Wu, B.; Heidelberg, A.; Boland, J. J. *Nat. Mater.* **2005**, *4*, 525–529.
(10) Zijlstra, P.; Tchebotareva, A. L.; Chon, J. W. M.; Gu, M.; Orrit, M. *Nano Lett.* **2008**, *8*, 3493–3497.
(11) Del Fatti, N.; Voisin, C.; Chevy, F.; Vallée, F.; Flytzanis, C. *J. Chem. Phys.* **1999**, *110*, 11484–11487.
(12) Hodak, J. H.; Henglein, A.; Hartland, G. V. *J. Chem. Phys.* **1999**, *111*, 8613–8621.
(13) Voisin, C.; Del Fatti, N.; Christofilos, D.; Vallée, F. *Appl. Surf. Sci.* **2000**, *164*, 131–139.
(14) Palpant, B.; Portales, H.; Saviot, L.; Lermé, J.; Prével, B.; Pellarin, M.; Duval, E.; Perez, A.; Broyer, M. *Phys. Rev. B* **1999**, *60*, 17107–17111.
(15) Chassaing, P.; Demangeot, F.; Combe, N.; Saint-Macary, L.; Kahn, M.; Chaudret, B. *Phys. Rev. B* **2009**, *79*, 155314.
(16) Varnavski, O.; Ramakrishna, G.; Kim, J.; Lee, D.; Goodson, T. *J. Am. Chem. Soc.* **2010**, *132*, 16–17.
(17) Alayan, R.; Arnaud, L.; Bourgey, A.; Broyer, M.; Cottancin, E.; Huntzinger, J. R.; Lermé, J.; Vialle, J. L.; Pellarin, M.; Guiraud, G. *Rev. Sci. Instrum.* **2004**, *75*, 2461–2470.
(18) Pérez, A.; Mélinon, P.; Dupuis, V.; Jensen, P.; Prével, B.; Tuaillon, J.; Bardotti, L.; Martet, C.; Treilleux, M.; Broyer, M.; Pellarin, M.; Vialle, J.; Palpant, B.; Lermé, J. *J. Phys. D: Appl. Phys.* **1997**, *30*, 709–721.
(19) Voisin, C.; Del Fatti, N.; Christofilos, D.; Vallée, F. *J. Phys. Chem. B* **2001**, *105*, 2264–2280.
(20) Burgin, J.; Guillon, C.; Langot, P. *Appl. Phys. Lett.* **2005**, *87*, 211916.
(21) Arbouet, A.; Voisin, C.; Christofilos, D.; Langot, P.; Del Fatti, N.; Vallée, F.; Lermé, J.; Celep, G.; Cottancin, E.; Gaudry, M.; Pellarin, M.; Broyer, M.; Maillard, M.; Pileni, M.; Treguer, M. *Phys. Rev. Lett.* **2003**, *90*, 177401.
(22) Juvé, V.; Scardamaglia, M.; Maioli, P.; Crut, A.; Merabia, S.; Joly, L.; Del Fatti, N. D.; Vallée, F. *Phys. Rev. B* **2009**, *80*, 195406.
(23) Nelet, A.; Crut, A.; Arbouet, A.; Del Fatti, N.; Vallée, F.; Portalés, H.; Saviot, L.; Duval, E. *Appl. Surf. Sci.* **2004**, *226*, 209–215.
(24) Voisin, C.; Christofilos, D.; Del Fatti, N.; Vallée, F. *Physica B* **2002**, *316-317*, 89–94.
(25) Lamb, H. *Proc. London Math. Soc.* **1882**, *s1–14*, 50–56.
(26) Dubrovskiy, V.; Morochnik, V. *Earth Phys.* **1981**, *17*, 494–504.
(27) Tamura, A.; Higeta, K.; Ichinokawa, T. *J. Phys. C: Solid State Phys.* **1982**, *15*, 4975–4991.
(28) Crut, A.; Maioli, P.; Del Fatti, N.; Vallée, F. *Phys. Chem. Chem. Phys.* **2009**, *11*, 5882–5888.
(29) Çağin, T.; Dereli, G.; Uludoğan, M.; Tomak, M. *Phys. Rev. B* **1999**, *59*, 3468–3473.
(30) Krauss, T.; Wise, F. *Phys. Rev. Lett.* **1997**, *79*, 5102–5105.
(31) Cheng, W.; Ren, S.; Yu, P. *Phys. Rev. B* **2003**, *68*, 193309.
(32) Ramirez, F.; Heyliger, P.; Rappé, A.; Leisure, R. *Phys. Rev. B* **2007**, *76*, 085415.
(33) Combe, N.; Chassaing, P.; Demangeot, F. *Phys. Rev. B* **2009**, *79*, 045408.

DOI: 10.1021/nl100604r | *Nano Lett.* **2010,** *10,* 1853–1858